J. Magn. Soc. Jpn., **40**, 132-136 (2016)

<Paper>

Preparation of YCo_5 and $GdCo_5$ Ordered Alloy Epitaxial Thin Films on Cu(111) Underlayer

Makoto Yamada, Yusuke Hotta, Mitsuru Ohtake,
Masaaki Futamoto, Fumiyoshi Kirino*, and Nobuyuki Inaba**

Faculty of Science and Engineering, Chuo University, *1-13-27 Kasuga, Bunkyo-ku, Tokyo 112-8551, Japan*
*Graduate School of Fine Arts, Tokyo University of the Arts, *12-8 Ueno-koen, Taito-ku, Tokyo 110-8714, Japan*
**Faculty of Engineering, Yamagata University, *4-3-16 Jyonan, Yonezawa, Yamagata 992-8510, Japan*

$Y_{17}Co_{83}$ and $Gd_{17}Co_{83}$ (at. %) alloy thin films are prepared on Cu(111) underlayers epitaxially grown on MgO(111) substrates at a substrate temperature of 500 °C by molecular beam epitaxy. The growth behavior and the film structure are investigated by *in-situ* reflection high-energy electron diffraction and X-ray diffraction. YCo_5 and $GdCo_5$ ordered alloy crystals epitaxially grow on the Cu underlayers. The epitaxial films consist of two (0001) variants whose orientations are rotated around the film normal by 30° each other. The epitaxial orientation relationships are (YCo_5 or $GdCo_5$)(0001)[$1\bar{1}00$] ∥ Cu(111)[$11\bar{2}$] (type A) and (YCo_5 or $GdCo_5$)(0001)[$11\bar{2}0$] ∥ Cu(111)[$11\bar{2}$] (type B). The volume ratios of two variants, $V_{\text{type A}}:V_{\text{typeB}}$, in YCo_5 and $GdCo_5$ films are estimated to be 65:35 and 72:28, respectively. The long-range order degrees of YCo_5 and $GdCo_5$ films are respectively determined to be 0.63 and 0.65. These ordered alloy films show perpendicular magnetic anisotropies reflecting the magnetocrystalline anisotropies of YCo_5 and $GdCo_5$ crystals.

Key words: YCo_5, $GdCo_5$, ordered alloy, epitaxial thin film, perpendicular magnetic anisotropy

1. Introduction

Magnetic thin films with the easy magnetization axis perpendicular to the substrate surface and with the uniaxial magnetocrystalline anisotropy energy (K_u) greater than 10^7 erg/cm^3 have been investigated for applications like future recording media with the areal density exceeding 1 Tb/in^2. A bulk $SmCo_5$ ordered alloy material with RT_5-type (R: rare earth metal, T: transition metal) structure (Fig. 1) shows K_u of 1.1 × 10^8 erg/cm^3 along the c-axis.[1)] (0001)-oriented $SmCo_5$ polycrystalline[2–7)] and epitaxial[8–10)] films have been prepared on Cu,[2–5,8,9)] Ru,[6,7,10)] and Ru-Cr[7)] underlayers.

The Sm and Co sites in $SmCo_5$ structure can be replaced with other R and T elements, respectively. In our previous studies, $SmFe_5$[11–13)] and $SmNi_5$[11,14)] ordered alloy epitaxial films were prepared on Cu(111) underlayers by using a molecular beam epitaxy (MBE) system equipped with a reflection high-energy electron diffraction (RHEED) facility. The crystallographic properties during formations of SmT_5 alloy films can be investigated by *in-situ* RHEED.

Ferromagnetic ordered alloys consisting of Co and R other than Sm with RT_5 structure such as YCo_5 and $GdCo_5$ also show K_u values greater than 10^7 erg/cm^3. However, there are few reports on the formations of (0001)-oriented RCo_5 epitaxial films. In the present study, $Y_{17}Co_{83}$ and $Gd_{17}Co_{83}$ (at. %) materials are deposited on Cu(111) underlayers. The growth behavior and the film structure are investigated.

2. Experimental Procedure

Thin films were deposited on polished MgO(111) single-crystal substrates by using an MBE system with the base pressure lower than 7 × 10^{-9} Pa. Pure Y (99.9%) and Gd (99.9%) metals were evaporated by electron beam heating, while pure Co (99.9%) and Cu (99.9999%) materials were evaporated by using Knudsen cells.

The film layer structures were $Y_{17}Co_{83}$(20 nm)/Cu(20 nm)/MgO(111) and $Gd_{17}Co_{83}$(20 nm)/Cu(20 nm)/MgO(111). MgO substrates were heated at 500 ºC for 1 hour before film formation to obtain clean surfaces. 20-nm-thick Cu underlayers were deposited on the substrates. The epitaxial orientation relationships between Cu underlayer and MgO substrate were Cu(111)[$11\bar{2}$] ∥ MgO(111)[$11\bar{2}$] and Cu(111)[$\bar{1}\bar{1}2$] ∥ MgO(111)[$11\bar{2}$]. $Y_{17}Co_{83}$ and $Gd_{17}Co_{83}$ films of 20 nm thickness were formed by co-evaporation of Y and Co or Gd and Co materials. The film composition was confirmed by energy dispersive X-ray spectroscopy to be within 17 ± 2 at. % R (R = Y or Gd), which is nearly the RCo_5 stoichiometry. The substrate temperature during film formation was kept constant at 500 °C.

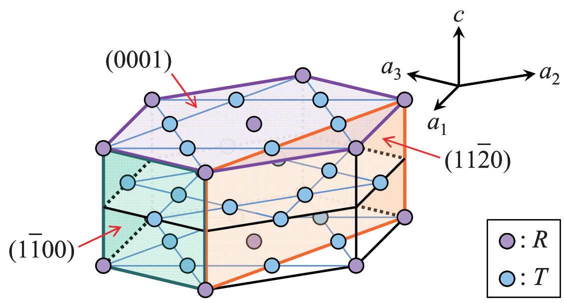

Fig. 1 Schematic diagram of RT_5 structure.

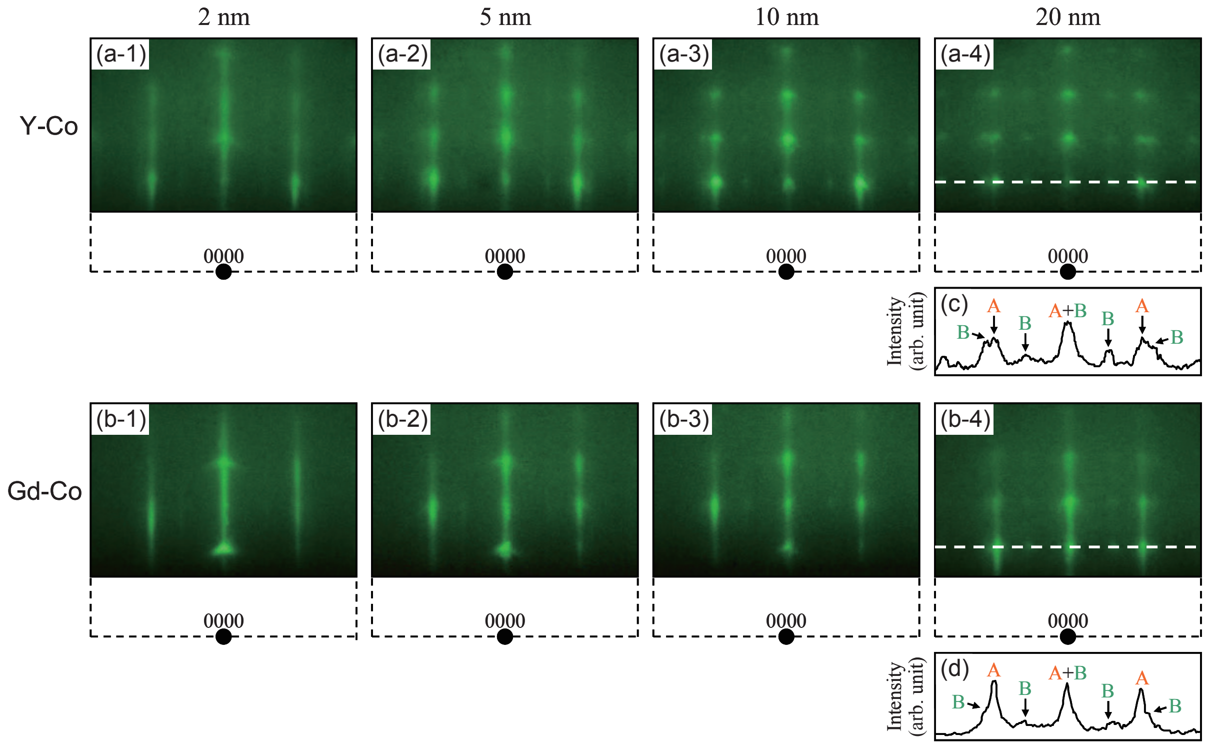

Fig. 2 [(a), (b)] RHEED patterns observed during formations of (a) $Y_{17}Co_{83}$ and (b) $Gd_{17}Co_{83}$ films on Cu(111) underlayers at 500 °C. The film thicknesses are [(a-1), (b-1)] 2, [(a-2), (b-2)] 5, [(a-3), (b-3)] 10, and [(a-4), (b-4)] 20 nm. The incident electron beam is parallel to MgO[$11\bar{2}$] (∥ Cu[$11\bar{2}$], [$\bar{1}\bar{1}2$]). The intensity profiles of (c) and (d) are measured along the white dotted lines in (a-4) and (b-4), respectively.

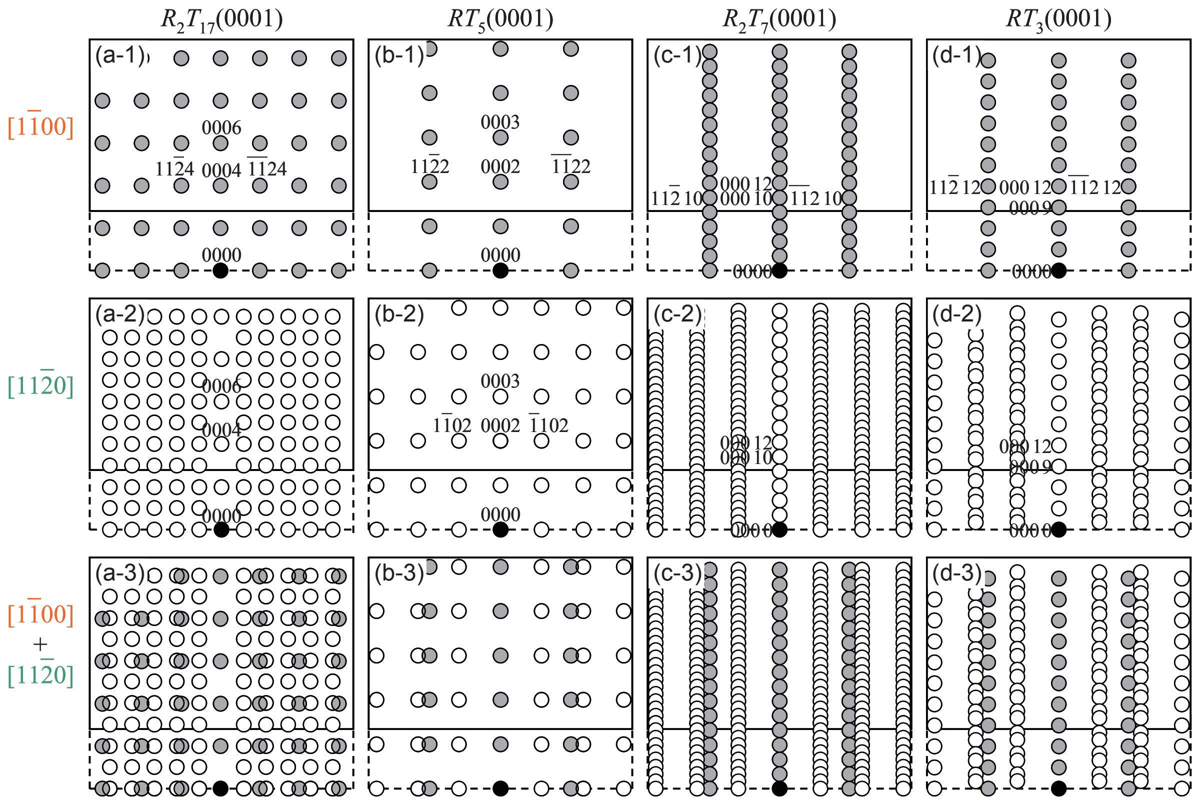

Fig. 3 [(a-1)–(d-1), (a-2)–(d-2)] Schematic diagrams of RHEED patterns simulated for hexagonal (a) R_2T_{17}, (b) RT_5, (c) R_2T_7, and (d) RT_3 ordered alloy crystals of (0001) orientation by using the lattice constants of bulk R_2T_{17} (a/2= 0.42 nm, c/2 = 0.40 nm), RT_5 (a =0.50 nm, c = 0.40 nm), R_2T_7 (a = 0.50 nm, c/9 = 0.40 nm), and RT_3 (a = 0.50 nm, c/6 = 0.40 nm) crystals. The incident electron beam is parallel to (a-1)–(d-1) [$1\bar{1}00$] or (a-2)–(d-2) [$11\bar{2}0$]. Schematic diagrams of (a-3)–(d-3) are drawn by overlapping (a-1)–(d-1) and (a-2)–(d-2), respectively.

The surface structure during film deposition was observed by RHEED. The resulting film structure was investigated by $2\theta/\omega$-scan out-of-plane, $2\theta\chi/\varphi$-scan in-plane, and β-scan pole-figure X-ray diffractions (XRDs) with Cu-Kα radiation (λ = 0.15418 nm). The magnetization curves were measured by superconducting quantum interference device (SQUID) magnetometry.

3. Results and Discussion

Figures 2(a) and (b) show the RHEED patterns of $Y_{17}Co_{83}$ and $Gd_{17}Co_{83}$ films deposited on Cu(111) underlayers observed by making the incident electron beam parallel to MgO[$11\bar{2}$] (|| Cu[$11\bar{2}$], [$\bar{1}\bar{1}2$]). Figure 3 shows the schematic diagrams of RHEED patterns simulated for hexagonal R_2T_{17}, RT_5, R_2T_7, and RT_3 ordered crystals of (0001) orientation. A clear RHEED pattern corresponding to the diffraction pattern simulated for RT_5(0001) surface [Fig. 3(b-3)] starts to be observed from the beginning of deposition and it remains unchanged until the end of film formation for both films. $Y_{17}Co_{83}$ and $Gd_{17}Co_{83}$ epitaxial films with RT_5 ordered structure are obtained. The observed RHEED patterns are analyzed to be an overlap of two reflections, as shown by the symbols, A and B, in the RHEED intensity profiles of Figs. 2(c) and (d). The crystallographic orientation relationships are thus determined as follows,

(YCo_5, $GdCo_5$)(0001)[$1\bar{1}00$] || Cu(111)[$11\bar{2}$], [$\bar{1}\bar{1}2$] || MgO(111)[$11\bar{2}$], (type A)

(YCo_5, $GdCo_5$)(0001)[$11\bar{2}0$] || Cu(111)[$11\bar{2}$], [$\bar{1}\bar{1}2$] || MgO(111)[$11\bar{2}$]. (type B)

The epitaxial films consist of two types of (0001) variant whose orientations are rotated around the film normal by 30° each other, which is similar to the growth of $SmCo_5$ film on Cu(111) underlayer.[8,9]

The lattice misfit values of YCo_5 and $GdCo_5$ crystals with respect to Cu underlayer are respectively –3.4% and –2.9% in the A-type orientation relationship, whereas those are +11.5% and +12.2% in the B-type relationship. Here, the mismatches are calculated by using the lattice constants of bulk YCo_5 (a_{YCo_5} = 0.4937 nm),[15] $GdCo_5$ (a_{GdCo_5} = 0.4963 nm),[15] and Cu (a_{Cu} = 0.3615 nm)[16] crystals. Although there are fairly large mismatches in the cases of B-type YCo_5 and $GdCo_5$ variants, epitaxial growth is taking place. The intensity of RHEED spot from A-type variant is stronger than that from B-type variant for both materials [Figs. 2(c), (d)]. The nucleation of A-type variant with smaller lattice misfits seems to be favored.

In order to investigate the volume ratio of two types of variant, β-scan pole-figure XRD was carried out. Figure 4 shows the β-scan XRD patterns of $Y_{17}Co_{83}$ and $Gd_{17}Co_{83}$ films measured by fixing the tilt and diffraction angles of (α, $2\theta B$) at (45°, 30.5°), where YCo_5{$1\bar{1}01$} and $GdCo_5${$1\bar{1}01$} reflections are expected to be detectable. Twelve {$1\bar{1}01$} reflections, which originate from the two types of variant, are observed with 30º separation for both films. The volume ratios of A-type to B-type variant in $Y_{17}Co_{83}$ and $Gd_{17}Co_{83}$ films are estimated from the integrated intensities of {$1\bar{1}01$} reflections to be 65:35 and 72:28, respectively. It is revealed that the volume ratio of A-type variant is larger than that of B-type variant.

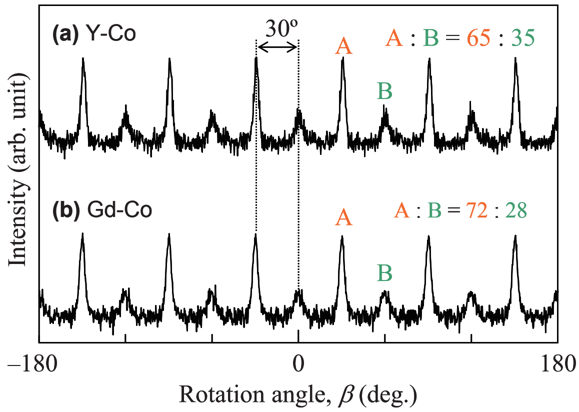

Fig. 4 β-scan pole-figure XRD patterns of (a) $Y_{17}Co_{83}$ and (b) $Gd_{17}Co_{83}$ films deposited on Cu(111) underlayers measured by fixing the (α, $2\theta B$) values at (45°, 30.5°). The intensity is shown in linear scale.

Figures 5(a-1) and (b-1) show the out-of-plane XRD patterns of $Y_{17}Co_{83}$ and $Gd_{17}Co_{83}$ films, respectively. RT_5(0001) superlattice and RT_5(0002) fundamental reflections are clearly observed for both films. The out-of-plane XRD confirms the formations of YCo_5 and $GdCo_5$ ordered phases. Long-range order degree, S, is estimated by comparing the intensities of superlattice and fundamental reflections. The intensity (I) is proportional to structure factor and the complex conjugate (FF^*), Lorentz-polarization factor (L), and absorption factor (A).[17] $F_{(0001)}$ and $F_{(0002)}$ are respectively $S(f_R - f_T)$ and $f_R + 5f_T$,[18] where f is the atomic scattering factor. Therefore, $I_{(0001)}/I_{(0002)}$ is expressed as

$$I_{RT_5(0001)}/I_{RT_5(0002)} = (FF^*LA)_{RT_5(0001)}/(FF^*LA)_{RT_5(0002)} = S^2[(f_R - f_T)^2]_{RT_5(0001)}/[(f_R + 5f_T)^2]_{RT_5(0002)} \times (LA)_{RT_5(0001)}/(LA)_{RT_5(0002)}. \quad (1)$$

By solving this equation, S is given as

$$S = [I_{RT_5(0001)}/I_{RT_5(0002)}]^{1/2} \times (f_R + 5f_T)_{RT_5(0002)}/(f_R - f_T)_{RT_5(0001)} \times [L_{RT_5(0002)}/L_{RT_5(0001)}]^{1/2} \times [A_{RT_5(0002)}/A_{RT_5(0001)}]^{1/2}. \quad (2)$$

The S values of $Y_{17}Co_{83}$ and $Gd_{17}Co_{83}$ films are respectively calculated to be 0.63 and 0.65.

Figures 5(a-2) and (b-2) show the in-plane XRD

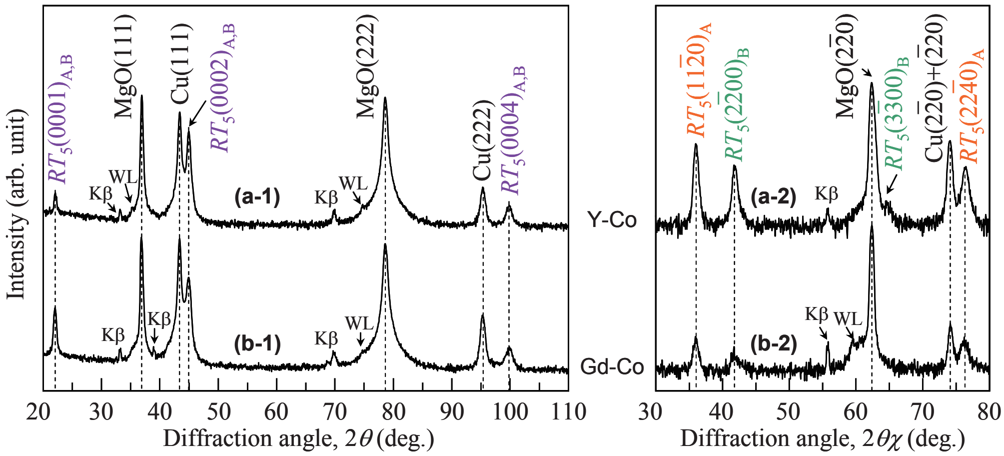

Fig. 5 [(a-1), (b-1)] Out-of-plane and [(a-2), (b-2)] in-plane XRD patterns of (a) $Y_{17}Co_{83}$ and (b) $Gd_{17}Co_{83}$ films deposited on Cu(111) underlayers. The scattering vector of in-plane XRD is parallel to MgO[$1\bar{1}0$]. The small reflections noted as Kβ and WL are due to Cu-Kβ and W-Lα radiations included in the X-ray source, respectively. The intensity is shown in logarithmic scale.

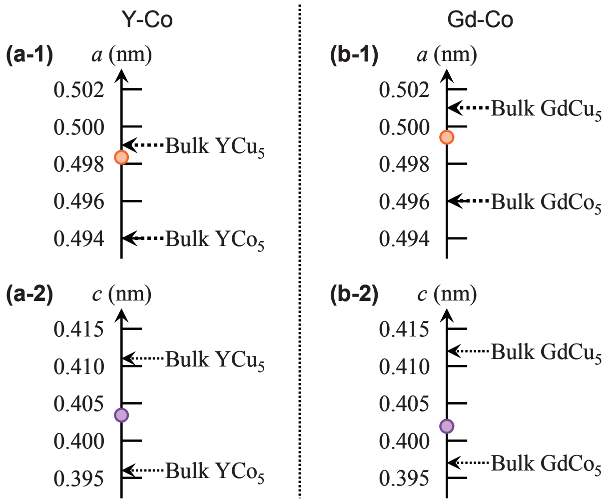

Fig. 6 Lattice constants of [(a-1), (b-1)] *a* and [(a-2), (b-2)] *c* of (a) $Y_{17}Co_{83}$ and (b) $Gd_{17}Co_{83}$ films deposited on Cu(111) underlayers.

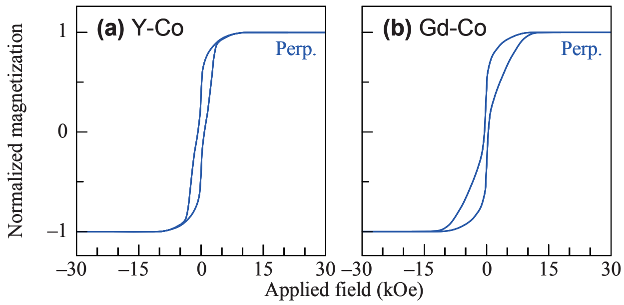

Fig. 7 Magnetization curves of (a) $Y_{17}Co_{83}$ and (b) $Gd_{17}Co_{83}$ films deposited on Cu(111) underlayers.

patterns measured by making the scattering vector parallel to MgO[$1\ \bar{1}\ 0$]. $RT_5(11\bar{2}0)$ and $RT_5(22\bar{4}0)$ reflections from A-type variant and $RT_5(2\bar{2}00)$ and $RT_5(3\bar{3}00)$ reflections from B-type variant are recognized for both films. The in-plane XRD confirms the epitaxial orientation relationship determined by RHEED.

Figure 6 shows the lattice constants, *a* and *c*, of $Y_{17}Co_{83}$ and $Gd_{17}Co_{83}$ films, which are respectively estimated from the peak position angles of $RT_5(22\bar{4}0)$ and $RT_5(0004)$ reflections. Here, the lattice constants of bulk YCo_5, $GdCo_5$, $Y_{0.8}Cu_{5.4}$, and $GdCu_5$ crystals are cited from Refs. 15, 19, and 20. The *a* and *c* values of $Y_{17}Co_{83}$ and $Gd_{17}Co_{83}$ films are between those of bulk YCo_5 and $Y_{0.8}Cu_{5.4}$ crystals and between those of bulk $GdCo_5$ and $GdCu_5$ crystals, respectively. It is reported that Cu atoms of underlayer diffuse into Sm-Co film and partially substitute the Co site in $SmCo_5$ structure forming an alloy compound of $Sm(Co,Cu)_5$.[4,5] The dissolution of Cu atom into Sm-Co alloy is known to stabilize RT_5 ordered structure.[21–23] In the present case, Cu atoms are considered to have diffused from the underlayers into the $Y_{17}Co_{83}$ and $Gd_{17}Co_{83}$ films forming alloy compounds of $Y(Co,Cu)_5$ and $Gd(Co,Cu)_5$. It is necessary to confirm the element distribution by using a chemical analysis method.

Figure 7 shows the magnetization curves of $Y_{17}Co_{83}$ and $Gd_{17}Co_{83}$ films measured by applying the magnetic field along the perpendicular direction. These films are easily magnetized, which seems to be reflecting the easy magnetization axis of YCo_5 and $GdCo_5$ ordered alloy crystals.

4. Conclusion

$Y_{17}Co_{83}$ and $Gd_{17}Co_{83}$ thin films are deposited on Cu(111) underlayers at 500 °C. The film growth behavior and the detailed film structure are investigated by RHEED and XRD. YCo_5 and $GdCo_5$ ordered alloy epitaxial films of (0001) orientation are obtained. The films consist of two types of (0001) variant whose orientations are rotated around the film normal by 30° each other. The S values of YCo_5 and $GdCo_5$ films are estimated to be 0.63 and 0.65, respectively. Cu atoms are considered to have diffused from the underlayers into the YCo_5 and $GdCo_5$ films and substitute the Co sites in YCo_5 and $GdCo_5$ structures forming alloy compounds of $Y(Co,Cu)_5$ and $Gd(Co,Cu)_5$. These ordered alloy films show perpendicular magnetic anisotropies reflecting the magnetocrystalline anisotropies of YCo_5 and $GdCo_5$ crystals.

Acknowledgments Authors thank Prof. Hirohiko Sato Chuo University for SQUID measurements. A part of this work was supported by JSPS KAKENHI Grant Numbers 25420294 and 26820117 and Chuo University Grant for Special Research.

References

1) K. J. Strnat: *Handbook of Ferromagnetic Materials* (Elsevier Science B. V., New York, 1988).
2) J. Sayama, T. Asahi, K. Mizutani, and T. Osaka: *J. Phys. D*, **37**, L1 (2004).
3) S. Takei, A. Morisako, and M. Matsumoto: *J. Magn. Magn. Mater.*, **272–276**, 1703 (2004).
4) J. Sayama, K. Mizutani, T. Ariake, K. Ouchi, and T. Osaka: *J. Magn. Magn. Mater.*, **301**, 271 (2006).
5) Y. K. Takahashi, T. Ohkubo, and K. Hono: *J. Appl. Phys.*, **100**, 053913 (2006).
6) I. Kato, S. Takei, X. Liu, and A. Morisako: *IEEE Trans. Magn.*, **42**, 2366 (2006).
7) X. Liu, H. Zhao, Y. Kubota, and J. -P. Wang: *J. Phys. D.*, **41**, 232002 (2008).
8) Y. Nukaga, M. Ohtake, F. Kirino, and M. Futamoto: *IEEE Trans. Magn.*, **44**, 2891 (2008).
9) M. Ohtake, Y. Nukaga, F. Kirino, and M. Futamoto: *J. Cryst. Growth*, **311**, 2251 (2009).
10) M. Seifert, V. Neu, and L. Schultz: *Appl. Phys. Lett.*, **94**, 022501 (2009).
11) M. Ohtake, O. Yabuhara, Y. Nukaga, F. Kirino, and M. Futamoto: *J. Appl. Phys.*, **107**, 09A708 (2010).
12) O. Yabuhara, M. Ohtake, Y. Nukaga, F. Kirino, and M. Futamoto: *J. Phys.: Conf. Ser.*, **200**, 082026 (2010).
13) T. Yanagawa, M. Ohtake, F. Kirino, and M. Futamoto: *EPJ Web Conf.*, **40**, 06007 (2013).
14) M. Yamada, Y. Hotta, T. Yanagawa, M. Ohtake, F. Kirino, and M. Futamoto: *IEEE Trans. Magn.*, **50**, 2101604 (2014).
15) H. Ido, M. Nanjo, and M. Yamada: *J. Appl. Phys.*, **75**, 7140 (1994).
16) D. N. Batchelder and R. O. Simmons: *J. Appl. Phys.*, **36**, 2864 (1965).
17) B. D. Cullity: *Elements of X-Ray Diffraction* (Addison-Wesley, Massachusetts, 1956).
18) M. Ohtake and M. Futamoto: *J. Magn. Soc. Jpn.*, **39**, 205 (2015).
19) Y. C. Chuang, C. H. Wu, and Y. C. Chang: *J. Less-Common Met.*, **84**, 201 (1982).
20) J. M. Barandiaran, D. Gignoux, J. M. Rodriguez Fernandez, and D. Schmitt: *Physica B*, **154**, 293 (1989).
21) F. Hofer: *IEEE Trans. Magn.*, **6**, 221 (1970).
22) K. Kamio, Y. Kimura, T. Suzuki, and Y. Itayama: *Trans. Jpn. Inst. Met.*, **14**, 135 (1973).
23) A. J. Perry: *J. Less-Common Met.*, **51**, 153 (1977).

Received Feb. 23, 2015; Revised Mar. 31, 2016; Accepted May 26, 2016